Eur. Phys. J. B **43**, 187–193 (2005)
DOI: 10.1140/epjb/e2005-00041-7

THE EUROPEAN PHYSICAL JOURNAL B

Fermionic Ising glasses in magnetic transverse field with BCS pairing interaction

S.G. Magalhães[1,a] and F.M. Zimmer[1]

Departamento de Física, CCNE Universidade Federal de Santa Maria, Faixa de Camobi, Km 5, 97105-900 Santa Maria, RS, Brazil

Received 16 June 2004
Published online 25 February 2005 –

Abstract. We study a fermionic infinited-ranged Ising spin glass with a real space BCS interaction in the presence of an applied transverse field. The problem is formulated in the integral functional formalism where the $SU(2)$ spins are given in terms of bilinear combinations of Grassmann fields. The problem is solved within static approximation and the replica symmetry ansatz combined with previous approaches used to study the critical behavior of the quantum Ising spin glass in a transverse field and the spin glass Heisenberg model with BCS pairing. Our results show that the transverse field has strong effect in the phase boundary of the spin glass phase and the PAIR phase in which there is a long range order corresponding to formations of pairs. The location of the tricritical point in the PAIR phase transition line is also affected.

PACS. 05.50.+q Lattice theory and statistics (Ising, Potts, etc.) – 64.60.Cn Order-disorder transformations; statistical mechanics of model systems

1 Introduction

Theoretical studies in recent years have been investigating the interplay between superconductivity (SC) and spin glass (SG) [1–5] which has been found in several strongly correlated electron systems, such as heavy fermions [6] and cuprate superconductors [7]. However, the experimental evidences for these correlated systems have showed a quite complex situation. For instance, the heavy fermion superconductor $U_{1-x}M_xPd_2Al_3$ (M = La, Y, Th) [6] shows a sequence of magnetic and Non-Fermi Liquid (NFL) ground states. In particular, when the content of La is increased, an antiferromagnetic phase is replaced by a SG which is suppressed to $T = 0$ K at $x = 0.75$. After the Quantum Critical Point (QCP), there is NFL region and at $x = 1$ appears superconductivity.

Some approaches have proposed that disorder itself can be the source of deviation of the Fermi Liquid behavior. For heavy fermions, for instance, the so called Kondo disordered model (KDM) [8] describes a distribution of Kondo temperature T_K given origin to the NFL behaviour. Castro-Neto et al. [9] relates the NFL effects to the presence of an inhomogeneous Griffith's phase. In an earlier work, it has been shown a NFL behavior near to the QCP in a transition between a metallic-paramagnet and a metallic-spin glass [10]. But, there is also the suggestion that the presence of QCP itself can be a source of a new class of excitations, which spread its effects even at finite temperatures leading to a breakdown of the Fermi liquid theory [11].

However, little consideration has been given to describe how the phase boundaries between superconductivity and spin glass are modified when at low temperature, besides the presence of thermal fluctuations, the quantum fluctuations start to become important. Some of the models previously mentioned [2,4] have addressed the phase transition problem between SG and superconductivity. Nevertheless, in those references there is no mechanism able to tune quantum fluctuations.

In particular, the model in reference [2] has been derived from a model introduced by Nass et al. [12] to deal with conventional superconductors doped with magnetic impurities. This model is an *s-d* exchange interaction between the magnetic impurities together with a conventional BCS interaction between the conducting electrons. When the conduction electrons are integrated by a perturbation expansion to second order in J_{sd} (the exchange interaction), the resulting effective model consists of the RKKY interaction with a pairing interaction between localized fermions. If the coupling J_{ij} between the localized magnetic moments is assumed to be random Gaussian distributed, one has a model to study the phase boundaries between SG and a phase where there is spin pairing [2].

The functional integral machinery, where the SU(2) spins have been represented by bilinear combination of

[a] e-mail: ggarcia@ccne.ufsm.br

the Grassmann variables, has been the suitable method used [2] to study the mentioned effective model in its Ising version. Combined with replica trick and the static approximation, it has allowed finding the Grand-Canonical potential in terms of the spin glass and the PAIR order parameters. The last phase corresponds to a long range order where there is pairs formation in the sites that occurs when the sites are double occupied [13]. In the half-filling situation, the results have showed a phase diagram temperature T/J versus g/J (g is the strength of the pairing interaction and J is the variance of J_{ij}) where one can find a spin glass phase for low temperature and small g. If g is increased, one gets a phase transition at $g = g_1(T)$ where there is a PAIR phase. The nature of the transition line is complex presenting a tricritical point (T_{tc}, g_{tc}).

Further investigation studied the pairing-spin glass competition replacing the fermionic Ising in the cited effective model by the Heisenberg model with an applied magnetic field H_z within the same framework of references [2] and [14]. The results have showed that the transition to the PAIR phase depends on the replica diagonal spin glass order parameter (which is associated with the susceptibility) even at higher temperatures than the freezing temperature T_f. The region in temperature where the calculated line transition between the normal-paramagnetic (NORMAL) and the PAIR phases is first order becomes larger when H_z is increased. Nevertheless, the line transition between the SG and the PAIR phase has not been accessible in this work. Other interesting point about the infinite ranged quantum Heisenberg model in the presence of a field is that T_f is depressed when the field increases, but never reaches a QCP [3].

Corrections in the weak hopping limit to the Ising SG fermionic model in the presence of a local pairing interaction have been studied elsewhere [4]. The results show that those corrections essentially preserve the shape of the phase diagram obtained with no hopping. Therefore, one can consider the range of validity of this theory as covering the transition between poor conductors and superconductors.

It is known that in the infinite ranged Heisenberg model the SG transition is not destroyed by spin flipping mechanism cased by quantum fluctuations [15]. On the other hand, in the Ising model the tunneling part of the Heisenberg Hamiltonian is disregarded and the magnetic order occurs only along the z direction. One variant of these models is a quantum Ising spin glass in a transverse field Γ. In this the quantum fluctuations, tuned by Γ, are used to mimic the spin flipping mechanism in a Heisenberg-like coupling among the three spin components. Therefore Γ play the role of the spin flipping part of the Heisenberg model allowing to access the QCP [16].

Recently, the Ising SG alone has been investigated in the transverse field Γ. The functional integral approximation have been used [17] to deal with the noncommutativity of the spins operators which have been represented by bilinear combinations of Grassmann fields. There are two versions of SG fermionic problem. The first one, the operator S_i^z has four eigenvalues (two of them are non-magnetic). In the second model, the two vanishing eigenvalues are suppressed by a restraint. In both models, the freezing temperature decreases with increasing Γ until to reach a QCP at a critical value Γ_c. This sort of approach is a natural tool to study phase transitions in condensed matter problems where fermions experiment couplings such as superconductivity and Kondo effect [18].

Therefore, our aim in this work have been to investigate how the phase boundary between a PAIR phase (where there is pair formation) and the four-state fermionic spin glass (SG) is modified if there is spin flipping induced by the presence of the transverse field Γ allowing to access the QCP [16]. In order to solve the functional integral over the Grassmann fields contained in the partition function, the formalism of Nambu matrices and spinors has been used. We also have used the replica symmetric "ansatz", and therefore we have calculated the Almeida-Thouless line [19] to obtain the validity limit of this procedure. Finally, we find the Grand-Canonical potential and the saddle point equations for the order parameters in the half-filling limit.

One important approximation in the present work is the neglecting of time fluctuations (the static approximation) [15]. For infinite ranged quantum Ising spin glass, a simulational approach [20] has shown that for temperatures close to the freezing temperature T_f (when $\Gamma = 0$) the static approximation can be considered reliable. On the other hand, it is quite clear that the static approximation is unable to capture the fundamental low temperature dynamical behavior of the correlation functions [21]. Nevertheless, it has been shown that for M-component quantum rotor model, in the limit $M = \infty$, the critical line is given by zero-frequency mode [22]. This critical behaviour coincides with the Ising SG in transverse field [21]. Therefore, that is the ultimate justification for the use of the static approximation to find the phase boundary between SG and the PAIR phase for increasing transverse field which is the main purpose of the present work.

This paper is organized as follow. In Section 2, we introduce the model and perform calculations using the replica trick and the static approximation in order to find the Grand canonical potential and the saddle point order parameters equations. The behavior of the tricritical point in the transition line to the PAIR phase is obtained as a function of both Γ and g. In Section 3, phase diagrams are build up with solutions from the set of the order parameter equations in both situations, T/J versus g/J (for two values of Γ) and T/J versus Γ/J (for several values of g). It is also suggested a relationship between Γ and g which allow to see more clearly the role of quantum fluctuations in the interplay between SG and the PAIR phase. In the last section, we present our conclusions and final remarks.

2 General formulation

The model considered in this work was obtained by tracing out the conducting electrons degrees of freedom of a superconductor alloy [2], resulting in an effective BCS

pairing interaction among fermions and a random Gaussian interaction coupling the localized spins. In the resulting effective model we apply the transverse field term. Therefore, the Hamiltonian is

$$\hat{H} - \mu\hat{N} = -\sum_{i,j} J_{ij}\hat{S}_i^z\hat{S}_j^z - \sum_{i,j}\frac{g}{N}c_{i\uparrow}^\dagger c_{i\downarrow}^\dagger c_{j\downarrow}c_{j\uparrow} - 2\sum_j \Gamma\hat{S}_j^x - \mu\sum_j\sum_{s=\uparrow,\downarrow}\hat{n}_{js} \quad (1)$$

where the sum is over the N sites of a lattice. The coupling J_{ij} is an independent random variable with Gaussian probability distribution given by

$$P(J_{ij}) = \sqrt{\frac{N}{32\pi J^2}}\exp\left(-\frac{J_{ij}^2}{32J^2/N}\right). \quad (2)$$

The spin operators in equation (1) are defined (see Refs. [2,17]) as:

$$\hat{S}_j^z = \frac{1}{2}[\hat{n}_{j\uparrow} - \hat{n}_{j\downarrow}]\ ; \quad \hat{S}_j^x = \frac{1}{2}[c_{j\uparrow}^\dagger c_{j\downarrow} + c_{j\downarrow}^\dagger c_{j\uparrow}] \quad (3)$$

where the $c_{j\sigma}^\dagger$ ($c_{j\sigma}$) are fermions creation (destruction) operators, with $\sigma =\uparrow$ or $\downarrow$ indicating the spin projections, $\hat{n}_{j\sigma} = c_{j\sigma}^\dagger c_{j\sigma}$ is the number operator and μ is the chemical potential. The second term on the right side of the equation (1) is a BCS like interaction and corresponds to the mechanism that favors the double occupation of sites.

The Grand Canonical partition function is formulated in the functional integral formalism for fermions using the anticommuting Grassmann variable $\phi_{js}^*(\tau)$ and $\phi_{js}(\tau)$ (τ is the complex time). Therefore one has

$$\mathcal{Z} = \int D(\phi^*\phi)\ \exp\left[A_0 + A_{SG} + A_\Gamma + A_{BCS}\right] \quad (4)$$

where the actions A_0, A_{SG}, A_Γ, and A_{BCS} are the free part, the spin glass part, the transverse field part and the pairing part, respectively. The three first ones assume (after time Fourier transformation) the following forms:

$$A_0 = \sum_j\sum_\omega \underline{\phi}_j^\dagger(\omega)(i\omega + \beta\mu)\underline{\phi}_j(\omega), \quad (5)$$

$$A_{SG} = \sum_{ij}\beta J_{ij}S_i^z(\Omega)S_j^z(-\Omega), \quad (6)$$

$$A_\Gamma = \sum_j\sum_\omega \beta\Gamma\underline{\phi}_j^\dagger(\omega)\underline{\sigma}_1\underline{\phi}_j(\omega) \quad (7)$$

where $S_j^z(\Omega) = \frac{1}{2}\sum_\omega \underline{\phi}_j^\dagger(\omega+\Omega)\underline{\sigma}_3\underline{\phi}_{j\sigma}(\omega)$, with Matsubara's frequencies $\omega = (2m+1)\pi$ and $\Omega = 2m\pi$ ($m = 0, \pm1, \cdots$). In the equations (5)-(7) we have used the Spinors

$$\underline{\phi}_j(\omega) = \begin{bmatrix}\phi_{j\uparrow}(\omega)\\ \phi_{j\downarrow}(\omega)\end{bmatrix}; \quad \underline{\phi}_j^\dagger(\omega) = \left[\phi_{j\uparrow}^*(\omega)\ \phi_{j\downarrow}^*(\omega)\right] \quad (8)$$

and the Pauli matrices

$$\underline{\sigma}_1 = \begin{pmatrix}0 & 1\\ 1 & 0\end{pmatrix};\ \underline{\sigma}_2 = \begin{pmatrix}0 & -i\\ i & 0\end{pmatrix};\ \underline{\sigma}_3 = \begin{pmatrix}1 & 0\\ 0 & -1\end{pmatrix}. \quad (9)$$

The pairing action is given by

$$A_{BCS} = \sum_{ij}\sum_\Omega \rho_i^*(\Omega)\rho_j(\Omega) \quad (10)$$

with $\rho_j(\Omega) = \sum_\omega \phi_{j\downarrow}(-\omega)\phi_{j\uparrow}(\Omega+\omega)$.

In this paper we discuss the phase transition problem within the static approximation, therefore only the term with $\Omega = 0$ is kept in the sum over the Matsubara's frequencies in equations (6) and (10). For this reason, we can define $S_j \equiv S_j^z(0)$ and write the following expression for the pairing action

$$A_{BCS}^{st} = \frac{\beta g}{4N}\sum_{p=1,2}\left[\sum_{j,\omega}\underline{\phi}_j^{'\dagger}(\omega)\underline{\sigma}_p\underline{\phi}_j^{'}(\omega)\right]^2, \quad (11)$$

where the Nambu matrices have been introduced in the previous equation,

$$\underline{\phi}_j^{'}(\omega) = \begin{bmatrix}\phi_{j\uparrow}(\omega)\\ \phi_{j\downarrow}^*(-\omega)\end{bmatrix};\ \underline{\phi}_j^{'\dagger}(\omega) = \left[\phi_{j\uparrow}^*(\omega)\ \phi_{j\downarrow}(-\omega)\right]. \quad (12)$$

The configurational averaged Grand Canonical potential per site can be found by using the replica formalism

$$\frac{\Omega}{N} = -\frac{1}{N\beta}\lim_{n\to0}\frac{\mathcal{Z}(n)-1}{n}. \quad (13)$$

The configurational averaged replicated partition function $\mathcal{Z}(n) = \langle\mathcal{Z}^n\rangle_{J_{ij}}$ becomes, after averaging over J_{ij},

$$\mathcal{Z}(n) = \int D(\phi_\alpha^*,\phi_\alpha)\exp\left\{\sum_\alpha[A_0^\alpha + A_\Gamma^\alpha] + \frac{\beta g}{4N}\sum_\alpha\sum_{p=1,2}\left(\sum_{j,\omega}\underline{\phi}_j^{'\alpha\dagger}(\omega)\underline{\sigma}_p\underline{\phi}_j^{'\alpha}(\omega)\right)^2 + \frac{8\beta^2J^2}{N}\sum_{\alpha,\beta}\left(\sum_j S_j^\alpha S_j^\beta\right)^2\right\}. \quad (14)$$

In the previous equation we introduce the replica index $\alpha = 1, 2, \cdots, n$. The linearization of equation (14) is obtained by using the Hubbard-Stratonovich transformation

$$\mathcal{Z}(n) = \mathcal{N}\int_{-\infty}^{\infty}\prod_\alpha d\eta_{R\alpha}d\eta_{I\alpha}\int_{-\infty}^{\infty}\prod_{\alpha\beta}dq_{\alpha\beta}\exp\Big\{-N \times\left(\beta g\sum_\alpha|\eta_\alpha|^2 + \frac{\beta^2J^2}{2}\sum_{\alpha\beta}q_{\alpha\beta}^2 - \ln\Lambda_\alpha(q_{\alpha\beta},\eta_\alpha)\right)\Big\}, \quad (15)$$

where was introduced replica dependent auxiliary fields $|\eta_\alpha|$ and $q_{\alpha\beta}$. In the equation (15) $\eta_\alpha = \eta_{R\alpha} - i\eta_{I\alpha}$, $\mathcal{N} = (\beta g N/\pi)^n(\beta^2 J^2 N/2\pi)^n$, where

$$\Lambda_\alpha(q_{\alpha\beta},\eta_\alpha) = \int \prod_{\alpha=1}^{n} D[\phi^{\alpha *}\phi^\alpha] \exp\left[\sum_\alpha (A_0^\alpha + A_\Gamma^\alpha) + 4\beta^2 J^2 \sum_{\alpha\beta} q_{\alpha\beta} S^\alpha S^\beta + \sum_\omega \underline{\phi}^{'\dagger\alpha}(\omega)\underline{\eta}_\alpha \underline{\phi}^{'\alpha}(\omega)\right], \quad (16)$$

with the matrix $\underline{\eta}_\alpha$ defined as:

$$\underline{\eta}_\alpha = \begin{pmatrix} 0 & \beta g \eta_\alpha \\ \beta g \eta_\alpha^* & 0 \end{pmatrix}. \quad (17)$$

The order parameter $|\eta_\alpha|$ introduced in the equation (15) corresponds to a long range order where there is double occupation of the sites [2], and $q_{\alpha\beta}$ is the spin glass order parameter.

In the present work we restrict the discussion to the replica symmetric ansatz, that considers

$$q_{\alpha\beta} = q; \quad q_{\alpha\alpha} = q + \bar{\chi} \quad (18)$$

where q is the spin glass order parameter and $\bar{\chi} = \frac{\chi}{\beta}$ (χ is the static susceptibility [23]). One can sum over the replica indices, which produces new quadratic terms that are linearized by introducing new auxiliary fields. Therefore, the functional integral becomes

$$\Lambda_\alpha(q_{\alpha\beta},\eta_\alpha) = \int_{-\infty}^{\infty} Dz \left[\int_{-\infty}^{\infty} D\xi \mathcal{I}(\xi,z,h)\right]^n \quad (19)$$

with $Dz = dz\frac{e^{-z^2/2}}{\sqrt{2\pi}}$, $D\xi = d\xi\frac{e^{-\xi^2/2}}{\sqrt{2\pi}}$, and

$$\mathcal{I}(\xi,z,h) = \int D[\phi^*\phi] \exp\left[\sum_\omega \underline{\phi}^\dagger(\omega)\underline{G}_1^{-1}(\omega)\underline{\phi}(\omega) + \sum_\omega \underline{\phi}^{'\dagger}(\omega)\ \underline{\eta}\ \underline{\phi}^{'}(\omega)\right] \quad (20)$$

where the matrix $\underline{G}_1^{-1}(\omega)$ is defined by $\underline{G}_1^{-1}(\omega_n) = i\omega_n + \beta\mu + \beta\Gamma\underline{\sigma}_1 + h\underline{\sigma}_3$ and the field $h = \beta J\sqrt{2\bar{\chi}}\xi + \beta J\sqrt{2q}z$.

In order to solve the integral in equation (20) which combines the elements of spinors and Nambu matrices, we can use a similar procedure already done in reference [3] which mixes the elements of the spinors and the Nambu matrices to write equation (20) as:

$$\mathcal{I}(\xi,z,h) = \int D[\phi^*\phi] \exp\left[\sum_\omega \underline{\Phi}^\dagger(\omega)\underline{G}^{-1}(\omega)\underline{\Phi}(\omega)\right] \quad (21)$$

where

$$\underline{\Phi}^\dagger(\omega) = \left[\ \phi_\uparrow^*(\omega)\ \phi_\downarrow^*(\omega)\ \phi_\downarrow(-\omega)\ \phi_\uparrow(-\omega)\ \right] \quad (22)$$

and

$$\underline{G}^{-1}(\omega) = \begin{pmatrix} i\omega+\zeta^+ & \beta\Gamma & \beta g\eta & 0 \\ \beta\Gamma & i\omega+\zeta^- & 0 & -\beta g\eta \\ \beta g\eta^* & 0 & i\omega-\zeta^+ & -\beta\Gamma \\ 0 & -\beta g\eta^* & -\beta\Gamma & i\omega-\zeta^- \end{pmatrix} \quad (23)$$

with $\zeta^\pm = \beta\mu \pm h$.

In the equation (21), the differential $D[\phi^*\phi]$ stands for $\prod_\omega \prod_{\sigma=\uparrow\downarrow} d\phi_\sigma^*(\omega)\ d\phi_\sigma^*(-\omega)\ d\phi_\sigma(\omega)\ d\phi_\sigma(-\omega)$. The functional integral over the Grassmann fields and the sum over the Matsubara frequencies can be readily performed with the result [2,3]:

$$\mathcal{I}(\xi,z,h) = \cosh\sqrt{(\beta\mu)^2 + (\beta g|\eta|)^2} + \cosh\sqrt{\Theta} \quad (24)$$

where $\Theta = h^2 + (\beta\Gamma)^2$.

The results obtained in equation (24) can be used in the equation (19) that allow us to rewrite the equation (15). Therefore, the saddle point method (see Eq. (13)) give us the Grand Canonical potential as

$$\frac{\beta\Omega}{N} = \beta g\eta^2 + \frac{\beta^2 J^2}{2}\bar{\chi}(\bar{\chi}+2q) - \int_{-\infty}^{\infty} Dz \ln I_a(z) \quad (25)$$

where

$$I_a(z) = \cosh\beta g\eta + \int_{-\infty}^{\infty} D\xi \cosh\sqrt{\Theta} \quad (26)$$

with the chemical potential fixed to ensure that we are in the half-filling situation. From now, the parameter η is used instead of $|\eta|$. The saddle point equations for order parameters that follow from equation (25) are:

$$\eta = \frac{1}{2}\int_{-\infty}^{\infty} Dz \frac{\sinh(\beta g\eta)}{I_a(z)}\ , \quad (27)$$

$$q = \int_{-\infty}^{\infty} Dz \left[\frac{\int_{-\infty}^{\infty} D\xi\ \frac{h\ \sinh\sqrt{\Theta}}{\sqrt{\Theta}}}{I_a(z)}\right]^2\ , \quad (28)$$

$$\bar{\chi} = \int_{-\infty}^{\infty} Dz \frac{I_b(z)}{I_a(z)} - q\ , \quad (29)$$

where

$$I_b(z) = \int_{-\infty}^{\infty} D\xi \left(\frac{\beta^2\Gamma^2\sinh\sqrt{\Theta}}{\Theta^{\frac{3}{2}}} + \frac{h^2\cosh\sqrt{\Theta}}{\Theta}\right). \quad (30)$$

The solution with replica symmetric is unstable at low temperature. Therefore, it is necessary to find the region in temperature where the Almeida-Thouless eigenvalue [19] λ_{AT} becomes negative, which is given by:

$$\lambda_{AT} = 1 - 2(\beta J)^2 \int_{-\infty}^{\infty} Dz \left(\frac{I_a(z)I_b(z) - I_c^2}{I_a(z)}\right)^2. \quad (31)$$

In the equation (31) $I_c(z)$ is

$$I_c(z) = \int_{-\infty}^{\infty} D\xi \frac{h\sinh\sqrt{\Theta}}{\sqrt{\Theta}}. \quad (32)$$

The Landau expansion of the Grand Canonical potential in powers of the two parameters η and q allow us to locate the second order line transition in the problem. Therefore, from equations (25–26):

$$\beta\Omega = \sum_{j=0}^{3} f_j(\eta, \bar{\chi}, \beta) q^j \tag{33}$$

where $\bar{\chi}(q, \eta, \beta)$ is the solution of the saddle point equation, that was rewrite in powers of q as:

$$\bar{\chi} = \bar{\chi}_0 + \bar{\chi}_1 q + \bar{\chi}_2 q^2. \tag{34}$$

Introducing equation (34) into equation (33), and expanding the coefficients f_j in powers of q and η, we obtain the following result:

$$\frac{\beta\Omega}{N} = \frac{\beta^2 J^2}{2}\bar{\chi}_0^2 - \ln(K_0) + A_2 q^2 + A_3 q^3 + B_2\eta^2 + B_4\eta^4 \tag{35}$$

with

$$A_2 = -\frac{\beta^2 J^2}{2!} + \beta^4 J^4 \bar{\chi}_0^2, \quad A_3 = -\frac{8\beta^6 J^6}{3}\bar{\chi}_0^3, \tag{36}$$

$$B_2 = \beta g - \frac{\beta^2 g^2}{2! K_0}, \tag{37}$$

$$B_4 = \frac{\beta^4 g^4}{4! K_0}\left(\frac{3}{K_0} - 1 + \frac{3J^2\bar{\chi}_0}{g^2}\left.\frac{\partial^2\bar{\chi}}{\partial\eta^2}\right|_{\eta=0}\right), \tag{38}$$

where $K_0 \equiv K(\eta = 0, \bar{\chi} = \bar{\chi}_0)$, $\bar{\chi}_0 \equiv \bar{\chi}(q = 0, \eta = 0, \beta)$, with $K(\eta, \bar{\chi}) = \cosh(\beta g \eta) + \int_{-\infty}^{\infty} D\xi \cosh\sqrt{\Delta}$,

$$\bar{\chi}(q = 0, \eta, \beta) = \frac{\int_{-\infty}^{\infty} D\xi \xi^2 \frac{\sinh\sqrt{\Delta}}{\sqrt{\Delta}}}{K(\eta, \bar{\chi})} \tag{39}$$

and $\Delta = 2\beta^2 J^2 \bar{\chi}\xi^2 + \beta^2\Gamma^2$.

The tricritical point is given when both coefficients B_2 and B_4 change the sign. In this condition we have solved numerically the equations (37) and (38) for several values of Γ_{tc} (the sub-index tc stands for the tricritical values of the temperature T, g and Γ). The results are shown in the phase diagrams (see Figs. 1, 2 and 3). Equation (38) is a correct result and S.G. Magalhães acknowledges a flaw in a previous publication [2].

3 Results

The numerical solutions of equations (27–29) allow one to construct two sorts of phase diagrams when Γ and g are independent parameters. The first one is T/J (T is the temperature) versus g/J (g is the strength of the pairing interaction) where the transverse field Γ/J is kept constant. The second one is T/J versus Γ/J with g being constant.

In the Figure 1, one can see the results obtained in a phase diagram T/J versus g/J for $\Gamma/J = 0$ and $\Gamma/J = 1$ (for numerical purposes $J = 1$). In the first case, we have obtained the same phase diagram already found in reference [2] with three distinct regions. The normal-paramagnetic (NORMAL) region at high T and small g (where $q = 0$ and $\eta = 0$). For $g > g_1(T)$ (see Sect. 1) one enters in the PAIR phase (where $q = 0$ and $\eta \neq 0$). Finally, for low T and small g, one has the phase transition to the spin glass phase (SG) at $T = T_f$ (T_f is the freezing temperature). This result is also obtained at half-filling situation in the reference [4]. When Γ is turned on, the freezing temperature decreases and the line transition $g = g_1(T)$ is displaced showing a dependence with Γ. Therefore, it is necessary to increase simultaneously the parameter g to find again solutions of the order parameters (see Eqs. (27–29)), which corresponds to the PAIR phase. The position of the tricritical point (T_{tc}, g_{tc}) also moves when Γ is increased and the first order line transition is enhanced. The first-order boundary, where there are multiple solutions, is obtained choosing between the NORMAL and PAIR solutions, or between the SG and PAIR solutions (for $T < T_f$), which minimizes the Grand Canonical potential (25). We also have obtained the behavior of the Almeida-Thouless (AT) eigenvalue λ_{AT} showing that for both values of Γ, the replica symmetric SG solution is unstable.

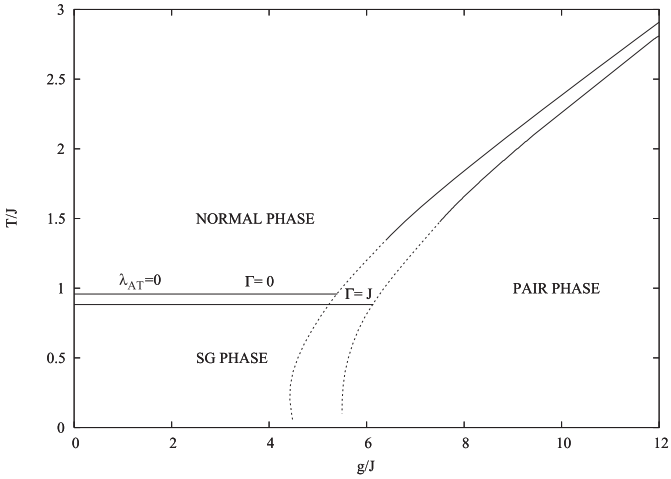

Fig. 1. Phase diagrams as a function of T/J and pairing coupling g/J for two values of Γ. Solid lines indicate second-order transition while dotted line indicate a first-order transition.

In Figure 2, the phase diagram is plotted T/J against Γ/J for several values of g. For $g = 0$ (see Fig. 2a), the corresponding phase diagram reproduces basically the results found in reference [17]. These results show that the freezing temperature T_f decreases (when Γ increases) towards to a QCP with $\Gamma_c = 2\sqrt{2}$. The entire SG region in the phase diagram is unstable (see the AT line in Fig. 2a). If g is turned on, which energetically favors the double occupation, the PAIR phase starts to appear. The existence of solution where $q = 0$ and $\eta \neq 0$ depends on the ratio Γ/g. For instance, in Figure 2b, one can find solutions for the order parameters which corresponds to the PAIR phase only for small values of Γ. In Figures 2c and Figure 2d, the strength g is increased and solutions with

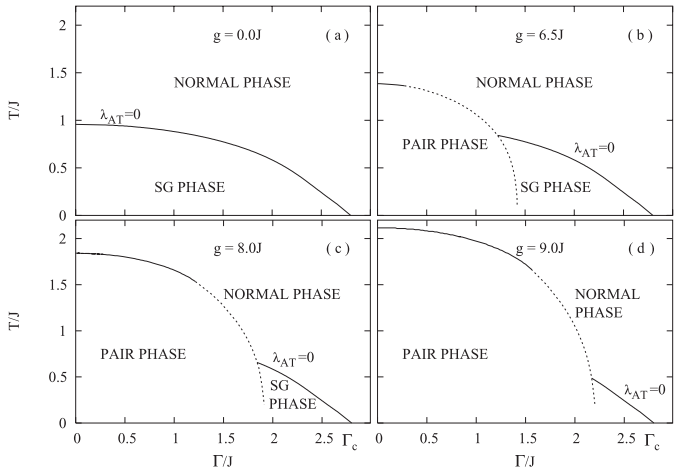

Fig. 2. Phase diagrams as a function of T/J and Γ/J for several fixed values of g/J: (a) $g = 0$, (b) $g = 6.5J$, (c) $g = 8J$, and (d) $g = 9J$. It is used the same convention as Figure 1 for the transition lines.

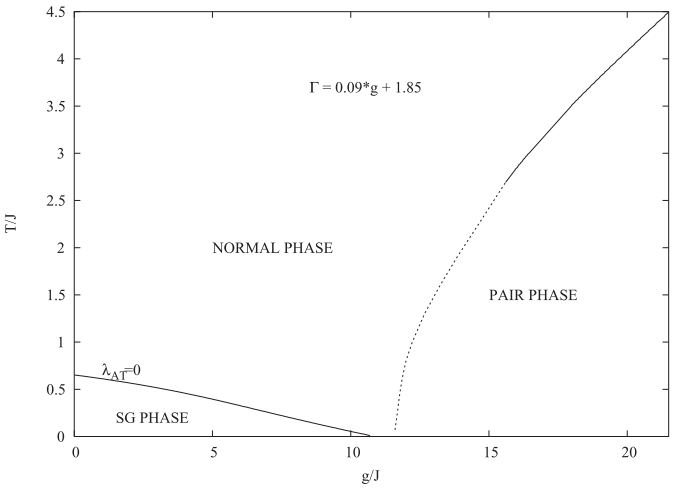

Fig. 3. Phase diagram build with a relationship between Γ and g. The dotted line indicates the first order transition while solid line the second order transition.

$\eta \neq 0$ starts to appear in a larger region of the diagram. Therefore, the sequence Figures 2a–2d shows clearly that it is requested greater values of g to the PAIR phase occupy a larger region than the SG phase. The QCP given by $\Gamma = \Gamma_c$ is the same as $g = 0$ and the SG phase remains unstable according to the calculated AT line.

However, one interesting effect in the interplay between SG and the PAIR phase can be seen if one considers that Γ and g are no longer independent parameters. Assuming the following relationship:

$$\Gamma = \alpha g + \Gamma_0. \tag{40}$$

As a justification of equation (40), one should recall the derivation of the effective model (see Eq. (1)) given in the Appendix of the reference [2]. The *s-d* exchange part, after the integration of the conducting electrons, originates the pairing interaction as well as the RKKY coupling between the localized spins.

The results have been shown in Figure 3 in a diagram T/J versus g/J. The position of the QCP (g_c) and the tricritical point (T_{tc}, g_{tc}) is very sensitive to the choice of the factors α and Γ_0. These factors have been adjusted to obtain a second order transition between the NORMAL and PAIR phases with the tricritical point located in the same scale of Figures 1–2. Therefore, for $\alpha = 0.09$ and $\Gamma_0 = 1.85$, one can see that as long as g increases (Γ also start to increase), the results show the freezing temperature T_f being depressed to zero at g_c. For $g > g_c$, the solutions for the order parameters indicate a NORMAL phase until one gets a line transition $g_1(T)$ between the NORMAL and the PAIR phases and $g_{tc} > g_c$. This phase diagram build with only one independent parameter (g) is more adequate to address the experiments.

4 Conclusions

In this work, we have investigated the competition between pairing formation in real space and spin glass order when tunneling is tuned by the transverse field Γ. We used the same framework of references [2,3,17], therefore, the partition function is obtained using the functional integral formalism and the spin operators are represented by Grassmann variables. One important point is the use of the static approximation and the symmetry replica "ansatz" in our approach. It is known that treatment which neglects the dynamical behavior of correlation functions is not correct at low temperatures. Nevertheless, our interest is mainly to capture the effects that appears on the phase boundaries when quantum tunneling is present due to the transverse field Γ. This procedure to find the phase boundaries is justified by the critical behaviour of quantum rotor model [22].

The main results can be seen in Figures 1, 2 and 3. The first two figures show that the pairing formation is not favored when the quantum tunneling is increased. At the same time, the temperature where is found the non-trivial spin glass ergodicity breaking decreases toward zero. For instance, in Figure 1, for the case $\Gamma = 0$ where it is found a SG phase, for small g (pairing interaction strength), below the freezing temperature $T_f = 0.95J$. The presence of transverse field ($\Gamma = J$) would favor the spin flipping destroying the double occupation of the sites. Therefore, it is necessary to increase g to find solutions for the order parameters where there is pairing long range order which corresponds to the PAIR phase. In that sense, the transverse field inhibit the pairing formation which makes the sites insensitives to a magnetic interaction. This results can be better seen in Figure 2 which show clearly that in order to found a PAIR phase when Γ is increased it is necessary greater values of the parameter g. The position of the tricritical point found in the PAIR line transition is quite sensitive to the presence of the transverse field. It moves up with Γ enlarging the first order transition region in the phase diagram.

In Figure 3, it is assumed a linear relationship between Γ and g (the strength of the pairing interaction)

given in equation (40). Therefore, the strength of spin flipping is now related with the strength of the pairing interaction. The first effect when g is increased is to lead the boundary line NORMAL-SG to a QCP at g_c. The pair formation is still inhibited even if g is kept increasing for values greater than g_c. The PAIR phase only appears at the line transition $g = g_1(T)$. This resulting phase diagram displays phase boundaries similar to the experimental one for $U_{1-x}La_xPd_2Al_3$ when $x > 0.5$ [6].

In conclusion, we have studied a fermionic representation of Ising spin glass (SG) in the presence of transverse magnetic field Γ together with local pairing interaction. We expect that results obtained in this model can contribute for the study of the interplay between spin glass and superconductivity in strongly correlated systems. Particularly, to describe the phase boundaries which is the main interest of this work. It should remarked that we have used the replica symmetry ansatz in the present work. There are results [4] indicating the Parisi replica permutation symmetry breaking affect the boundary between superconductivity and the SG phase. This is an indication that would be necessary to go beyond the replica symmetry solution in the present work. That will be subject for future work.

The numerical calculations were partially performed at LSC (Curso de Ciência da Computação, UFSM). SGM is grateful to Prof. Alba Theumann for useful comments. This work was partially supported by the Brazilian agencies FAPERGS (Fundação de Amparo à Pesquisa do Rio Grande do Sul) and CAPES (Coodenação de Aperfeiçoamento de Pessoal de Nivel Superior).

References

1. N. Hasselmann, A.H. Castro Neto, C. Morais Smith, Phys. Rev. B **69**, 014424 (2004)
2. S.G. Magalhães, A. Theumann, Eur. Phys J. B **9**, 5 (1999)
3. S.G. Magalhães, A.A. Schmidt, Phys. Rev. B **62**, 11686 (2000)
4. H. Feldmann, R. Opermann, Eur. Phys. J. B **10**, 429 (1999)
5. V.M. Galitski, A.I. Larkin, Phys. Rev. B **66**, 064526 (2002)
6. V.S. Zapf, R.P. Dickey, E.J. Freeman, C. Sirvent, M.B. Maple, Phys. Rev. B **65**, 024437 (2001); H. Spille, M. Winkelmann, U. Ahlheim, C.D. Bredl, F. Steglich, P. Haen, J.M. Mignot, J.L. Tholence, R. Tournier, J. Magn. Magn. Mater. **76/77**, 539 (1988)
7. F.C. Chou, N.R. Belk, M.A. Kastner, R.J. Biergenau, A. Aharony, Phys. Rev. Lett. **75**, 2204 (1995)
8. E. Miranda, V. Dobrosavljevic, Phys. Rev. Lett. **78**, 290 (1997); E. Miranda, V. Dobrosavljevic, Phys. Rev. Lett. **86**, 264 (2001)
9. A.H. Castro-Neto, B.A. Jones, Phys. Rev. B **62**, 14975 (2000)
10. A.M. Sengupta, A. Georges, Phys. Rev. B **52**, 10295 (1995)
11. P. Coleman, C. Pépin, Physica B, **383/389** 312 (2002); M. Continentino, Phys Rev. B **47**, 11587 (1993)
12. M.J. Nass, K. Levin, G. Grest, Phys. Rev. B **23**, 1111 (1981)
13. K.A. Penson, M. Kolb, Phys. Rev. B **33**, 1663 (1986); A.E. Sikkema, I. Affleck, Phys. Rev. B **52**, 10207 (1995)
14. Y.Y. Goldschmidt, Pik-Yin Lai, Phys. Rev. B **43**, 11434 (1991)
15. A.J. Bray, M.A. Moore, J. Phys. C **13**, L655 (1980)
16. A. Theumann, B. Coqblin, Phys. Rev. B **69**, 214418 (2004)
17. A. Theumann, A.A. Schmidt, S.G. Magalhães, Physica A **311**, 498 (2002)
18. A. Theumann, B. Coqblin, S.G. Magalhaães, A.A. Schimdt, Phys. Rev. B **63**, 54409 (2001); S.G. Magalhães, A.A. Schmidt, A. Theumann, B. Coqblin, Eur. Phys. J. B **30**, 419 (2002); S.G. Magalhães, A.A. Schmidt, F.M. Zimmer, A. Theumann, B. Coqblin, Eur. Phys. J. B **34**, 447 (2003)
19. J.R.L. de Almeida, D.J. Thouless, J. Phys. A: Math. Gen. **11**, 983 (1978)
20. D.R. Grempel, M.J. Rozemberg, Phys. Rev. Lett. **80**, 389 (1998)
21. J. Miller, D. Huse, Phys. Rev. Lett. **70**, 3147, (1993)
22. J. Ye, S. Sachdev, N. Read, Phys. Rev. Lett. **70**, 4011 (1993); N. Read, S. Sachdev, J. Ye, Phys. Rev. B **52**, 384 (1995)
23. A. Theumann, M. Vieira Gusmão, Phys. Lett. A **105**, 311 (1984)